Journal of
Water & Climate Change

IWA PUBLISHING

Journal of Water and Climate Change Vol 12 No 8, 3750 doi: 10.2166/wcc.2021.281

Hydrologic responses to climate and land-use/land-cover changes in the Bilate catchment, Southern Ethiopia

Hailu Gisha Kuma *, Fekadu Fufa Feyessa and Tamene Adugna Demissie

Jimma Institute of Technology, Jimma University, P. O. Box 378, Jimma, Ethiopia
*Corresponding author. E-mail: hailugisha@yahoo.com

HGK, 0000-0001-5755-888X; FFF, 0000-0001-8974-0328; TAD, 0000-0001-6750-8819

ABSTRACT

The likely effects of climate and land-use/land-cover (LULC) changes on hydrologic processes in Bilate catchment, Ethiopia were evaluated. The study emphasizes the evaluation of individual and combined impacts on hydrologic responses of climate and LULC changes. Climatic scenarios included a downscaled regional climate model from CORDEX-Africa. The CA–Markov model was used to project LULC. The results revealed that distinct changes on hydrologic responses occurred which follow the direction of climate and LULC changes. A 30.87% decline in rainfall resulted in about 4.09, 1.43 and 3.57% decline in runoff, groundwater and water yield, respectively. A rise in mean temperature by 1.3 °C resulted in a 7 and 0.8% increase in potential and actual evapotranspiration, respectively. Runoff, groundwater and water yield are projected to decrease by 11.24, 12.54 and 11.54%; however, potential and actual evapotranspiration are projected to increase by 19 and 14.7%, respectively, under combined climate and LULC changes. The joint effects of climate and LULC changes on hydrologic responses in the forthcoming were higher than the variation trend of climate or LULC change alone. Climate change compared with LULC change has a higher impact on hydrologic responses. The results obtained provide further insight into future water balance, and assistance in water resources planning and management.

Key words: Bilate catchment, climate change, LULC change, SWAT model, water balance

HIGHLIGHTS

- The study employed CA–Markov, regional climate and SWAT models.
- The projected change in temperature and rainfall impacts the hydrologic responses.
- Hydrologic responses follow the direction of climate change.
- Individual and combined impacts of climate and land-use/land-cover changes on hydrologic responses were evaluated.
- Potential and actual evapotranspiration are projected to increase, while runoff, groundwater and water yield are projected to decrease.

GRAPHICAL ABSTRACT

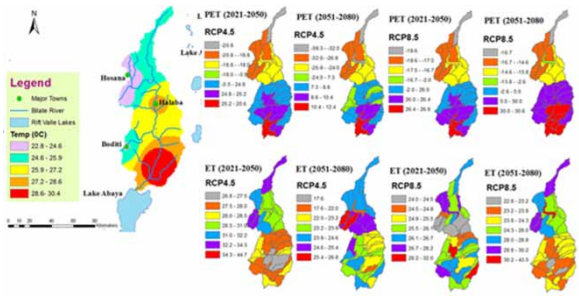

INTRODUCTION

Water managers and planners are facing substantial uncertainties in the future demand and availability of water. Land-use/land-cover (LULC) and climate changes and their probable hydrological effects are increasingly contributing to this uncertainty. LULC and climate changes are expected to alter the timing and magnitude of hydrological processes. LULC and climate changes are important factors causing combined impacts on catchment hydrologic processes.

Many studies from different parts of the world show that LULC and climate changes significantly impact hydrologic processes. For example, Liu *et al.* (2020) found that the combined effect of LULC and climate changes increased runoff by 0.22 m^3/s, in which LULC change caused the runoff increase by 0.07 m^3/s attributed to the decreased area of arable land and the increased area of urban land in the Coastal Basin, Northern China. Besides, four future hypothetical LULC scenarios and climate change simulation showed a decrease in streamflow by 11.8 and 26.72%, while sediment yield decreased by 7.54, 19.4, 11.1 and 9.01% in the Upper Ebonyi River watershed, Nsukka, South-East Nigeria (Ndulue & Mbajiorgn 2018). Other studies have discussed the impacts of LULC and climate changes on catchment hydrologic processes at different places (Li *et al.* 2009; Zuo *et al.* 2016; Bessah *et al.* 2020). Studies in Blue Nile Basin, Ethiopia indicated that water resources are vulnerable to both LULC and climate changes (Woldesenbet *et al.* 2018; Gebresilassie *et al.* 2020; Tigabu *et al.* 2020; Getachew *et al.* 2021; Negesse 2021; Teklay *et al.* 2021). Besides, a study at the Rift Valley Basin, Ethiopia showed that the combined effect of LULC and climate changes significantly decreases streamflow by 11.8% and increases evapotranspiration by 2.2% at Meki River Basin (Legesse *et al.* 2010).

To keep up water resources in the desired manner, it is important to predict and evaluate the future water balance tendencies at the catchment scale. Therefore, the assessment of anthropogenic activities on LULC and climate changes on hydrologic processes is highly desired, which requires effective hydrologic modeling. Hydrologic models have been advanced, as they provide comprehensive analysis between LULC, climate and water resources (Germer *et al.* 2009). Zhang *et al.* (2020) employed the SWAT model to evaluate the influence of LULC change on the hydrologic cycle, in Su-Mi-Huai, China investigated the response of surface runoff, recharge, and provided the basis for rational water resources planning. The soil and water assessment tool (SWAT) has been widely employed for the evaluation of impacts of LULC and climate changes on hydrologic processes (Shooshtari *et al.* 2017; Yin *et al.* 2017; Berihun *et al.* 2019; Lamparter *et al.* 2019).

In several previous studies, the impacts of changing climate on hydrologic processes are investigated by using downscaled regional climate model data in the SWAT model (Boru *et al.* 2019; Worner *et al.* 2019; Yan *et al.* 2019). Regional climate models at their finer resolution allow the simulation of local climate conditions in detail and provide future predictions. A coordinated regional climate downscaling experiment has been planned to simulate the climate of Africa based on a variety of climate regimes (Giorgi *et al.* 2009). Some countries are vulnerable to future climate change, for example Ethiopia is often cited as one of the most extreme examples (Conway & Schipper 2010). The expected effects in Omo Gibe Basin, Ethiopia are already having a profound effect on hydrology in the Omo River flows (Mohammed 2013). Despite the vulnerability to climate change, few attempts have been made to indicate water scarcity for different sectors.

Bilate catchment is found in the Rift Valley Basin, Ethiopia where small-scale irrigation projects are planned to improve the livelihoods of the growing population. In Bilate catchment, there are some districts whose population density exceeds six hundred individuals per kilometer square (CSA 2013; Adugna 2014). Population growth aggravates LULC change because of very high pressure on the land resources. Sloppy terrain areas and grazing fields were converted into cultivation lands in the catchment. As a result reduction in natural vegetation, soil erosion, sediment and nutrient loads to water bodies became common problems. In the catchment, there is high competition for irrigation water. A few state farms, individual investors and farmers use Bilate River and its tributaries without water management. Besides, subsistence farming in the catchment is exposed to fluctuating rainfall, and the growing population depends on limited land and water resources. The Ethiopian economy is rain-fed agriculture, which is heavily sensitive to climate variability and change (Zerga & Gebeyehu 2018). The short rainy season (February–May) crop of 2021 had completely failed due to the highest decline in February, March and April rainfall in the catchment. However, there is inadequate information about LULC and climate change effects on water resources in the catchment. Bilate catchment has been exposed to problems, and the result of this study would be important to supplement the water and LULC management strategies. Therefore, the aim of this study is intended to explore the combined and individual impacts of LULC and climate changes on the hydrologic responses in Bilate catchment, Ethiopia. LULC and climate change scenarios were used for hydrologic simulations using the SWAT model for two future periods.

MATERIALS AND METHODS

Study area

Bilate catchment covers 562,560 ha of land area and is located in the Rift Valley Lakes Basin, Ethiopia (Figure 1). It is bounded by Omo Gibe Basin to the west, Abiyata and Shala Lakes to the east. The catchment draws out across different climate zones ranging from the high to the lowlands of the Rift Valley. The altitude of the catchment ranges from 1,174 meters at Lake Abaya to 3,330 meters above sea level. The elevated terrains are the Ambarcho, Duguna, Mugo and Damota mountains which made the catchment undulating and characterized by steep slopes. Toward the center and the south, the morphology is quite gentle slopes. The Bilate River and its tributaries drain to Lake Abaya. Its maximum discharge is provided by most of the perennial streams from the western high lands of the catchment and the eastern intermittent streams provide fewer amounts.

Data source and methodology

A 30 m×30 m resolution DEM of Bilate catchment was downloaded from USGS at https://earthexplorer.usgs.gov site and used to delineate the watershed using SWAT and to analyze the drainage patterns of the land surface terrains. The data was projected to UTM zone 37 north on the spheroid of D-WGS 1984 datum (Figure 2(a)). The inclusive physico-chemical properties of soil are required by the SWAT model. A 250 m resolution of soil grids was assessed from the world digital soil map of the Food and Agricultural Organization (FAO 2002). The extraction was performed using ArcGIS 10.3 software. The classification used is based on the FAO classification system and customized in the way the SWAT model requires (Figure 2(b)). The dominant soils of this catchment include Vitric Andosols, Pellic Vertisols, Chromic Vertisols, Orthic

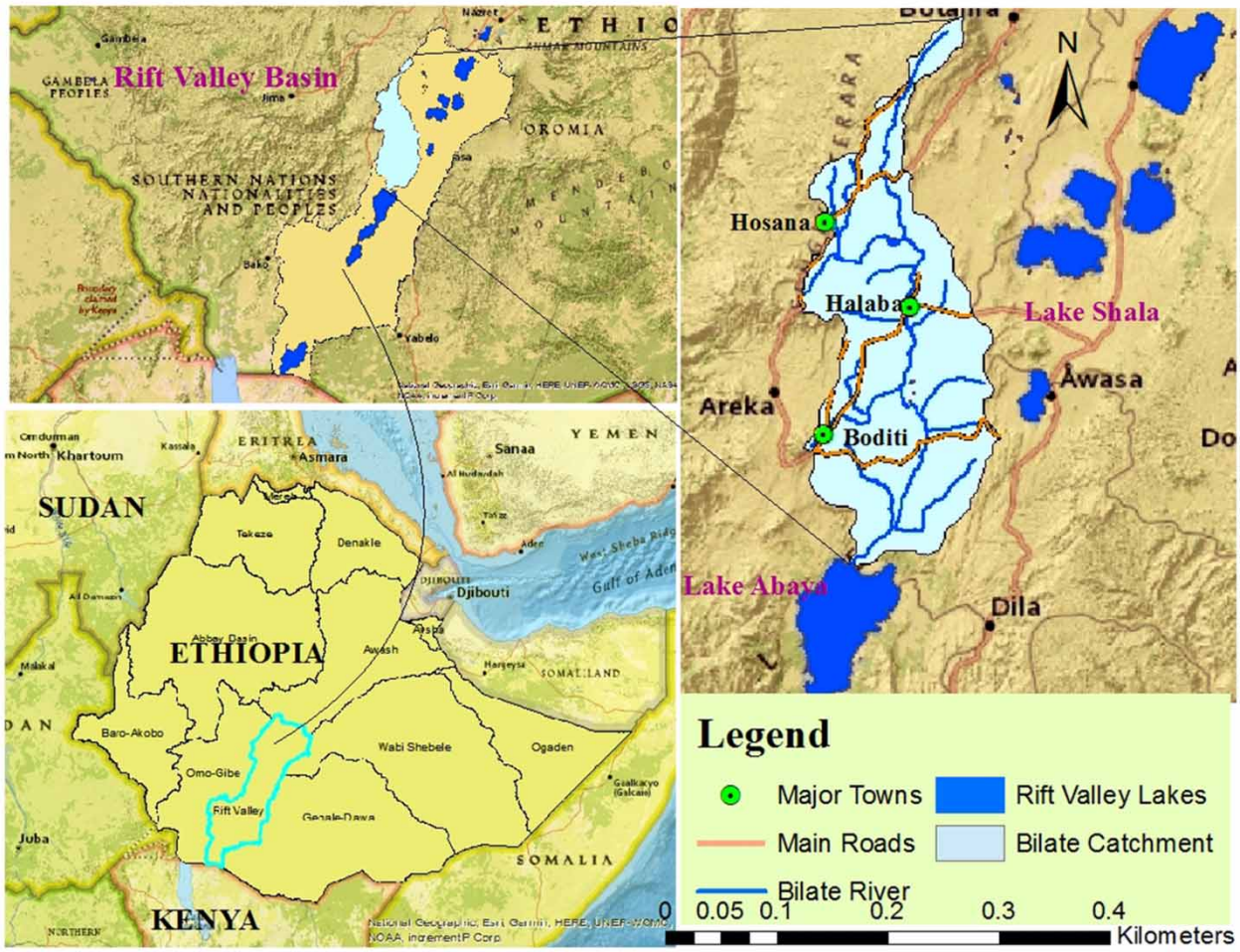

Figure 1 | Location map of the Bilate catchment.

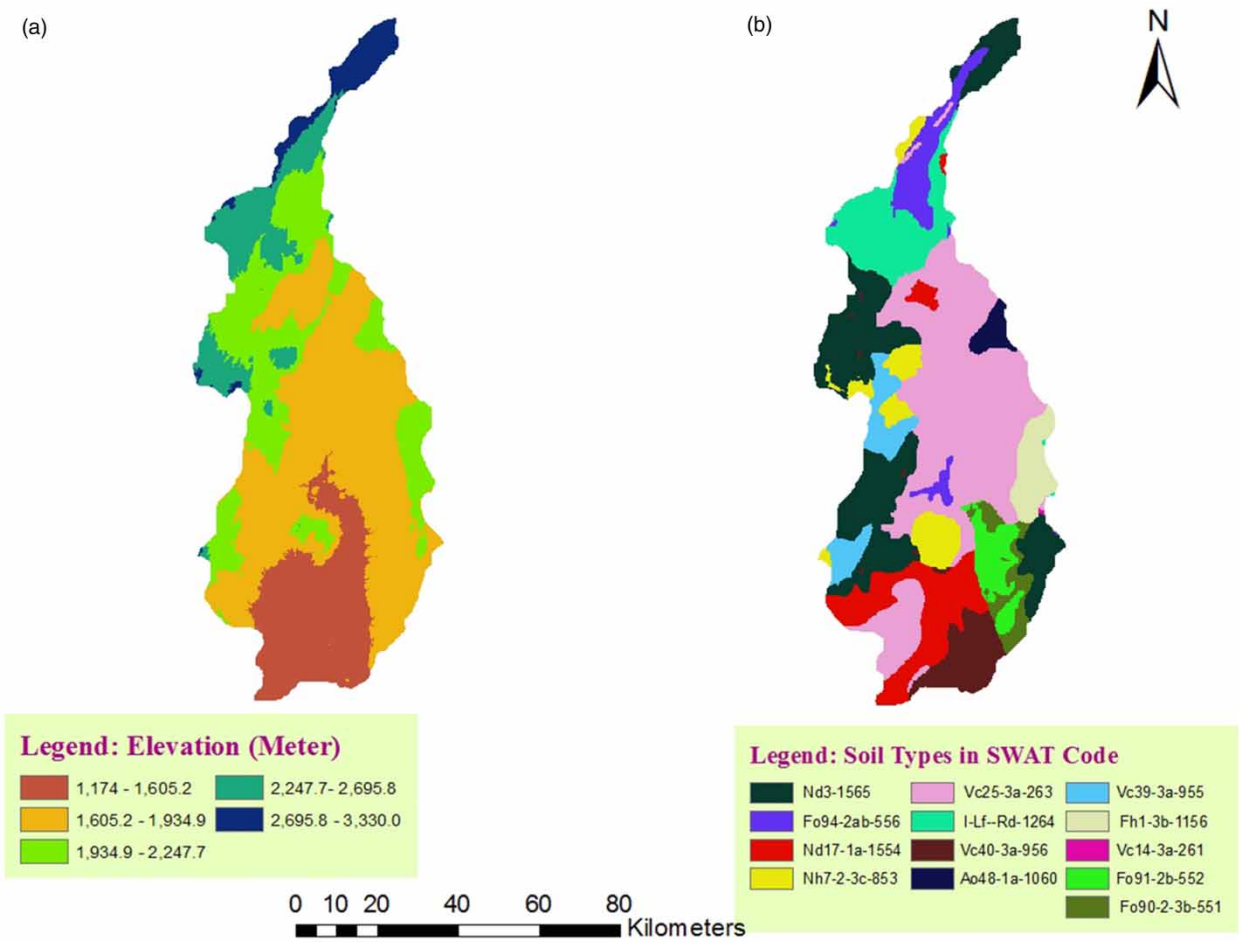

Figure 2 | DEM and soil map of Bilate catchment.

Solonchaks, Chromic Luvisols, Eutric Fluvisols, Eutric Nitisols and Dystric Nitisols rating at 31.8, 18.4, 9.9, 8.3, 5.7, 5.4, 4.8 and 4.2%, respectively; Eutric Regosols, Calcic Fluvisols, Calcaric Fluvisols, Luvic Phaeozems and Mollic Andosols rating at 3.6, 3.4, 3.1, 1.4 and 0.01%, respectively.

SWAT requires daily weather data for water balance simulation. Observed daily rainfall, temperature, humidity, wind speed and daily sunshine data from 1981 to 2017 were collected from the National Meteorological Agency of Ethiopia (NMSA 2019). Historical daily data of Bilate River flow gauge station near Halaba Kulito of the period 2006–2017 was used for calibration and validation. The data was obtained from the Ministry of Water, Irrigation and Energy of Ethiopia (MoWIE 2019). The gauging station was considered the biggest contributor to the Bilate River flow of the catchment.

The LULC maps of 1986, 2002 and 2018 were prepared by using Landsat images of TM, ETM+ and OLI, respectively, with the aid of ERDAS Imagine 2015 and Arc GIS 10.3. Six LULC classes of each map were identified (Figure 3). The classes are coded according to the SWAT database as water bodies (WATR), urban and built-up areas (URBN), grazing lands (PAST), forest lands/scattered (FRST), barren lands (BARR) and cultivation lands (AGRC). LULC evaluation result revealed the expansion of cultivation land, barren land, built-up areas and water body rating from 61.55 to 71.01%, 2.91 to 4.27%, 0.20 to 0.89% and 0.16 to 0.35% of the catchment area, respectively. However, the forest and grazing lands declined from 31.48 to 22.96% and 3.97 to 0.51%, respectively, in between 1986 and 2018. The overall image classification accuracies were 88.0, 89.33 and 91.67% for 1986, 2002 and 2018, respectively. K coefficients were 0.84, 0.86 and 0.89 for 1986, 2002 and 2018, respectively.

Land-use change modeling and validation

LULC change prediction was conducted by using the cellular automata and Markov chain (CA–Markov) model in IDRISI software (Nouri *et al.* 2014; Qiu & Lu 2018). The model is proficiently employed to simulate temporal and spatial

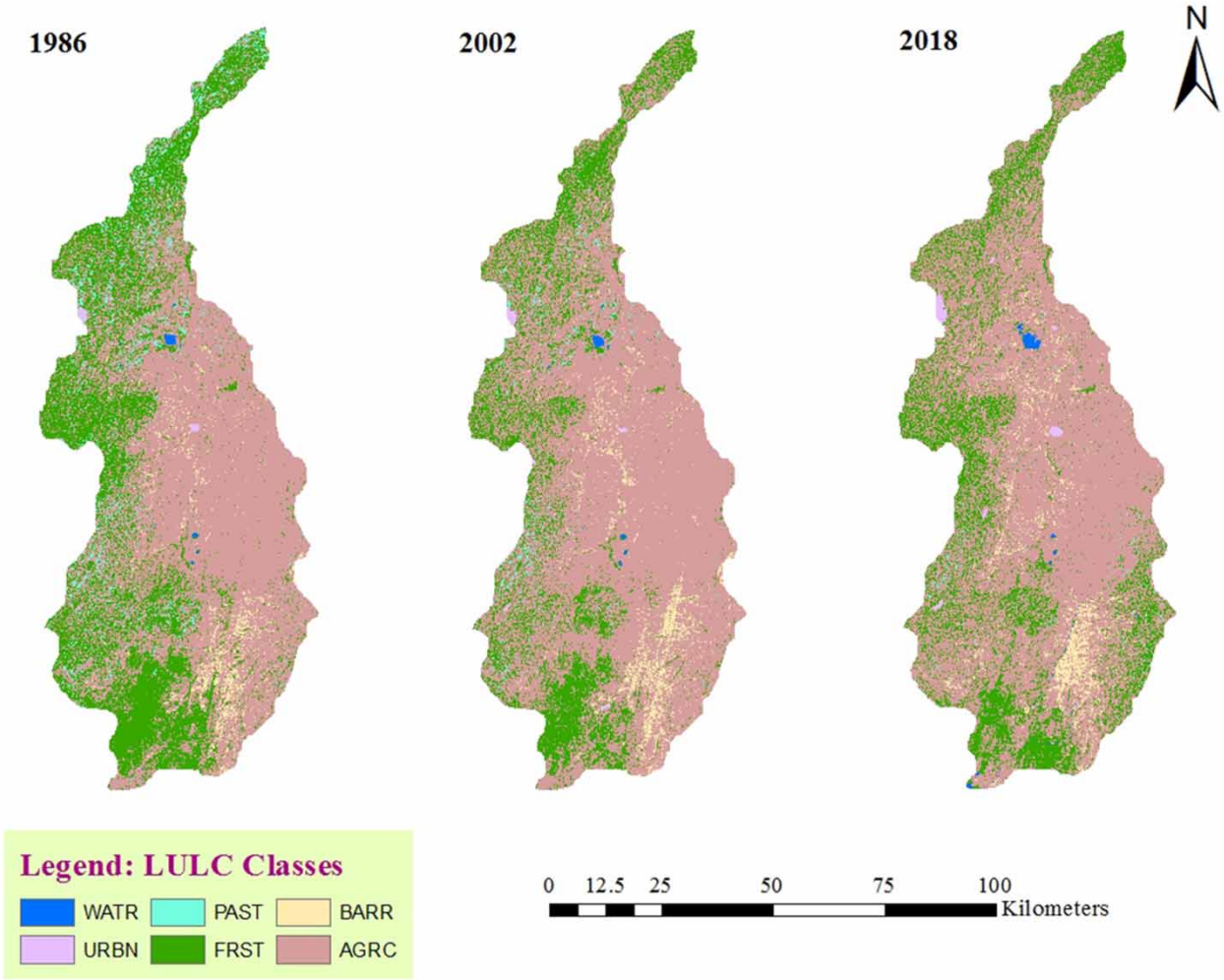

Figure 3 | LULC maps of 1986, 2002 and 2018 of the Bilate catchment.

land-use changes. The model recognizes spatial land-use distributions and transitions (Gidey *et al.* 2017). Temporally, the model forecasts change probability from one particular class to another class (Al-sharif & Pradhan 2014). LULC maps of 1986, 2002 and 2018 were used for land-use analysis in IDRISI 17.02 software. The procedure involves the following steps: transition probability matrix, transition area matrix and transition suitability maps. LULC maps of 2002 and 2018 were used in this procedure for calibration. The transition probability matrix contains the changing probability of an individual land-cover class to other classes, while the transitional area matrix contains the pixel number that is expected to change from each land-use class over the specified time frame (Eastman 2016). Suitability maps were developed for each LULC class based on potential driving factors with multi-criteria evaluation. Factors such as DEM (aspect, altitude and slope), urban centers, distance from streams and roads were utilized to generate suitability maps. Finally, the LULC maps for 2038 and 2058 were projected by using basic LULC maps, transition areas and transition suitability images.

Validation is the measure of the reliability of a model in predicting the future LULC by using datasets. LULC of 1986 and 2002 maps were used to simulate the 2018 LULC map. Markov transitions areas and transition suitability images were developed using 1986 and 2002 LULC maps. The simulated 2018 land-use map was compared with the reference 2018 land-use map using K indexes (Pan *et al.* 2017). The quantification and location errors are resolved by cause-dependent K-indexes such as K as overall accuracy of simulation (Kno), K for location (Klocation), K for standard (Kstandard) and K for stratum-level location (Klocationstrata) (Kim *et al.* 2011; Pontius & Millones 2011; Mosammam *et al.* 2016). The combination of K-indexes is considered for a comprehensive evaluation of the overall accuracy in the validation of the model. Kno measures the overall fraction of correctly classified versus expected values. Klocation evaluates the measure of spatial accuracy due to the correct

assignment of values between the simulated and reference maps. Kstandard estimates the proportion assigned correctly versus a proportion that is correct by chance. Klocationstrata quantifies spatial accuracy within predefined strata, and how well the grid cells are situated within the strata. The precision and consistency values of the κ coefficient below 0.4 indicates less, $0.4 \leq \kappa \leq 0.75$ is moderate and $\kappa > 0.75$ is a high level of consistency between the simulated and reference land-use maps (Viera & Garret 2005).

Climate change model

Regional climate model data extraction and bias correction

Regional climate model simulations for multi-period employed downscaling under the lateral boundary conditions are from a completely coupled GCM and components of the climate system (Castro *et al.* 2005). The downscaled regional climate model data were obtained from https://esg-dn1.nsc.lpu.se/projects/esgf.liu/cordex. The CORDEX-Africa model data at longitude 0.44° and latitude 0.44° horizontal resolution and a multi-model ensemble of regional climate models with their driving GCMs providing the boundary conditions were used in the study (Nikulin *et al.* 2012). Owing to the diversity of climate regimes and to improve simulations and projections, the coordinated regional climate downscaling experiment CORDEX-Africa was set (Giorgi *et al.* 2009). The model selection was built on the choice of likely variations in climatic means, changes in climatic limits and the model's ability to reproduce the past climate (Lutz *et al.* 2016). These five regional climate models with their driving GCMs employed CCLM4-ICHEC, RCA4-CanESM2, REMO2009-MPI, HIRHAM5-ICHEC and RACMO22T-ICHEC (Mascaro *et al.* 2015). The selected regional climate models were further evaluated using statistical parameters to check their association with observed data from the weather stations. Due to doubts in the model forecasts, it is necessary to assess the model's performance in simulating the climate in comparison to observations (Flato *et al.* 2013; Tinghai *et al.* 2013). The climate model data were evaluated against the observed rainfall and temperature data through the root-mean-square error (RMSE) and the Pearson correlation coefficient (r) (Chai & Draxler 2014). The association has been performed with the historical model data from 1981–2010 with that of observed data within the identical period. Climate parameters such as rainfall and temperature were evaluated for two weather stations. The r and RMSE between models and observed data of maximum temperature are in between 0.64 and 0.86, and 2.1 and 9.2, respectively. Similarly, the r and RMSE of minimum temperature are in between 0.45 and 0.63, and 2.2 and 5.10, respectively. Besides, the r and RMSE of rainfall are in between 0.55 and 0.81, and 4.7 and 11.5, respectively, of the models and observed data.

The downloaded regional climate model data were in the NetCDF file format. The regional climate model data of rainfall, minimum and maximum temperatures were extracted by ArcGIS 10.3 software through a multidimensional tool and NetCDF table view. The stations' data were extracted through their latitudes and longitudes. The bias is the long-term average difference between the observed and model data. Bias correction was employed on the regional climate model's rainfall and temperature in Bilate catchment.

Climate model data downloaded from CORDEX-Africa through RCP4.5 and RCP8.5 emission scenarios were used to project the future rainfall and temperature over Bilate catchment. An individual climate model is liable to uncertainties that may arise from climate models. To resolve this problem, the ensemble average of five climate models was used in the analysis of rainfall and temperature.

Precipitation correction

The power transformation algorithm has been used to correct the spatial distributional biases in rainfall outputs in regional climate models. The power transformation corrects both the mean and coefficient of variation to normalize peak daily and monthly rainfall amounts at rain gauge stations. This method was employed in Hare watershed, Southern Rift Valley of Ethiopia (Biniyam & Kemal 2017). Similarly, the power transformation was employed for the basin of the river Meuse upstream of Borgharen in the Netherlands (Leander & Buishan 2007); in the Rhine Basin, Western Europe (Terink *et al.* 2009). This method matches the coefficient of variations of the stations' and regional climate models' rainfall data. The daily rainfall quantity p converted to a modified rainfall amount P^* is given by the following equation (Leander & Buishan 2007; Leander *et al.* 2008):

$$P^* = aP^b \tag{1}$$

where a is the transformation coefficient and b is a scaling exponent. In this study, coefficients of variations (CV) of the observed rainfall data were matched with the climate model (RCM) rainfall data with some numerical iteration processes.

Temperature correction

The mean and standard deviation adjustment method was employed to correct the temperature. The mean and standard deviation adjustment is calculated according to the following equation (Leander & Buishan 2007):

$$Tc = \bar{T}_{\text{obs}} + \frac{Std_{\text{obs}}}{Std_{\text{model}}}(T_{\text{model}} - \bar{T}_{\text{model}}) \tag{2}$$

where T_c is the bias-corrected future temperature, $\bar{T}_{\text{obs}}$ is the mean observed temperature in the baseline period, $\bar{T}_{\text{model}}$ is the mean RCM temperature in the baseline period, T_{model} is the RCM temperature in the future period, Std_{obs} is the standard deviation of observed temperature in the baseline period and Std_{model} is the standard deviation of climate model temperature in the baseline period.

SWAT model

The physically-based, semi-distributed SWAT model was developed to simulate the effect of land-use management practices on hydrologic processes taking place in basins (Arnold *et al.* 1998). The water equilibrium approach of the SWAT model simulates surface runoff, infiltration, percolation, channel routing, shallow and deep aquifer flow. SWAT uses the water balance approach to simulate watershed hydrologic partitioning (Neitsch *et al.* 2011). The hydrologic routines replicated by the SWAT model are established on the water equilibrium equation:

$$SW_t = SW_0 + \sum_{i=1}^{t}(P_{\text{day}} - Q_{\text{sur}} - E_a - W_{\text{seep}} - Q_{\text{gw}}) \tag{3}$$

where SW_t is the last soil water content (mm), SW_{o} is the primary soil water content on the day i (mm), t is the time (days), P_{day} is the quantity of precipitation on the day i (mm), Q_{surf} is the quantity of surface runoff on the day i (mm), E_a is the quantity of evapotranspiration on the day i (mm), W_{seep} is the quantity of water entering the vadose zone from the soil profile on the day i (mm) and Q_{gw} is the quantity of return flow or base flow on the day i (mm). The SWAT run was performed on a daily climatic data basis. The data consist of rainfall, solar radiation, relative humidity, wind speed, minimum and maximum temperatures from two stations located in Bilate catchment.

Parameter sensitivity analysis, model calibration and validation

Model parameters exert the highest influence on model calibration and predictions. The models respond in a different way to different parameters, and as a result, the outputs become different. Model sensitivity is scrutiny of the change in model output per change in a parameter of input. Sensitivity analysis is one version of the SWAT model tool to show the mean relative sensitivity of the best parameters through SWAT-CUP (Feyereisen *et al.* 2007).

Model calibration is the adjustment of model parameters, within the recommended ranges, to optimize the simulated output so that it matches with the observed data. Calibration allows the provision of different parameters for the adjustment during operation. Validation is the process of testing the calibrated parameters with an independent set of observed data without further changes to parameters. Flow data collected at the gauging station near Halaba was used for Bilate River flow simulation for the period 2006–2017. The river flows from 2006–2017 were split into warm-up (2006–2008), calibration (2009–2014) and validation (2015–2017) periods. The Sequential Uncertainty Fitting version two (SUFI-2) algorithm set in SWAT-CUP 2012 was used during model calibration and validation (Abbaspour *et al.* 2007).

Model performance evaluation

The fitness of SWAT model simulation with the river flow was conveyed by statistics like the coefficient of determination (R^2) and the Nash–Sutcliffe simulation efficiency (NSE) (Nash & Sutcliffe 1970). Their values range from 0 to 1; the closer the value to 1, the higher the agreement between the simulated and the measured flows. R^2 describes the proportion of the

total variance in the observed and simulated data that can be explained by the model and given by the following equation:

$$R^2 = \frac{(\sum [Qsi - Qsi_{av}][Qob - Qob_{av}])^2}{\sum [Qsi - Qsi_{av}]^2 \sum [Qob - Qob_{av}]^2} \quad (4)$$

where, Qob is the observed/measured value; Qob_{av} is the average measured value. Qsi is the predicted value, and Qsi_{av} is the average predicted value.

NSE shows the degree of fitness of observed and simulated data and given by the following equation:

$$\text{NSE} = 1 - \frac{\sum (Qob - Qsi)^2}{\sum (Qob - Qob_{av})^2} \quad (5)$$

where Qob is the measured value, and Qob_{av} is the average measured value. Qsi is the predicted value. The measured, simulated and average values were measured in m^3/s. NSE shows how well the plot of observed versus simulated value fits the 1:1 line. The NSE and R^2 values are greater than 0.5 and 0.6, respectively, the simulated value is a better predictor than the mean measured value and is viewed as acceptable performance (Santhi *et al.* 2001).

Parameter uncertainty is caused by parameter non-uniqueness and input uncertainty as a result of errors in input data such as rainfall, land-use, soil-type and observed data. The model simulation uncertainty was quantified by 95% prediction uncertainty (95PPU) (Abbaspour *et al.* 2007). The quality of calibration and prediction uncertainty is judged based on the closeness of *p*-factor to 100% (all observations bracketed by the prediction uncertainty) and *r*-factor to 1 (achievement of a rather small uncertainty band) (Talebizadeh *et al.* 2009).

RESULTS AND DISCUSSION

Sensitivity analysis, model calibration, validation and performances

Sensitivity analysis

Model calibration requires the identification of key parameters and parameter precision. The sensitivity analysis of Bilate catchment by the SWAT model utilized 12 parameters. The global sensitivity analysis of a multiple regression system was employed against Nash–Sutcliffe objective function. Twelve parameters are found to be sensitive with relative sensitivity values, for example, runoff curve number to moisture condition II (CN2), groundwater 'revap' coefficient (GW_REVAP), effective hydraulic conductivity in the main channel (CH_K2), groundwater delay (GW_DELAY), deep aquifer percolation fraction (RCHRG_DP), baseflow recession constant (ALPHA_BF), threshold depth of water in the shallow aquifer for 'revap' to occur (REVAPMN), soil evaporation compensation factor (ESCO), threshold depth of water in the shallow aquifer required for return flow to occur (GWQMN), plant uptake compensation factor (EPCO), surface runoff lag coefficient (SURLAG), an available water capacity of the soil layer (SOL_AWC) and effective hydraulic conductivity in main channel alluvium (SOL_K). These sensitive parameters are considered the high effect on Bilate River flow during calibration and validation in SWAT-CUP (Table 1). The assessment of sensitive parameters was measured using the *t*-stat and *p*-values. The sensitive parameters were selected on the basis where the *t*-stat values are more sensitive for larger absolute *t*-stat values and *p*-values are closer to 0.

Flow calibration and validation

The calibration and validation were performed by using Bilate River flow at Halaba gauging station from 2009 to 2014 and 2015 to 2017, respectively. The periods were used for river flow calibration and validation by employing the 2018 LULC. The river flow was calibrated by auto-calibration and manual procedures. Model simulations during calibration and validation periods were evaluated on the monthly basis of the NSE and R^2. Based on procedures suggested by Moriasi *et al.* (2007), calibrated and validated river flows were agreeable at the monthly time scale. Peak flow values exhibited by observed and simulated flows during model calibration and validation. River flow calibration and validation were performed on a monthly basis. Six years for calibration and 3 years for validation were used. Flow hydrographs were derived to evaluate observed and simulated flow values for calibration and validation for 2018 LULC (Figure 4).

Table 1 | Flow sensitive parameters, fitted values, their *t*-stat and *p*-values

2018 LULC

Parameter	Range	Fitted	Parameter name	*t*-stat	*p*-value
r__CN2.mgt	35–98	37.6144	4:R__SOL_AWC(..).sol	6.388	0.000
v__GW_DELAY.gw	0–12	4.2500	5:R__SOL_Z(..).sol	6.651	0.000
r__GW_REVAP.gw	0–1	0.1507	6:R__SOL_K(..).sol	6.954	0.000
r__SOL_AWC().sol	0–1	0.4735	10:R__CH_N2.rte	6.966	0.000
r__SOL_Z().sol	0–3500	71.7500	12:R__CANMX.hru	7.278	0.000
r__SOL_K().sol	0–2000	1101.00	2:V__GW_DELAY.gw	7.514	0.000
r__SURLAG.bsn	0–12	8.8260	9:R__EPCO.hru	7.825	0.000
r__ESCO.hru	0.02–0.2	0.0145	8:R__ESCO.hru	8.880	0.000
r__EPCO.hru	0–1	0.3725	11:R__CH_K2.rte	9.356	0.000
r__CH_N2.rte	−0.01–1	0.5505	7:R__SURLAG.bsn	10.244	0.000
r__CH_K2.rte	0–500	94.2500	3:R__GW_REVAP.gw	10.715	0.000
r__CANMX.hru	0–100	87.1500	1:R__CN2.mgt	17.444	0.000

Hydrological model performances

The mean monthly simulated flows seem to have replicated the observed flows as shown in the calibration and validation results (Figure 4). The calibration result indicates that the SWAT model can capture the observed flow with R^2 and NSE of 0.79 and 0.71, respectively. Validation indicates R^2 and NSE of 0.81 and 0.73, respectively. Besides, *p*-factor and *r*-factor showed good agreement with 0.82 and 0.75 during calibration and 0.83 and 0.73 during validation, respectively. Both the calibration and validation indicate that the SWAT model achieved a relatively good fit between observations and simulations.

Land-use changes

Simulation of 2018 LULC

The LULC maps of 1986 and 2002 were used to simulate the LULC map of 2018 using the CA–Markov model. The 2018 map was compared with the simulated map 2018 to appraise the performance of the CA–Markov model using κ indexes. The model validation results on cause-dependent K indexes with K for overall accuracy (Kno), K for location (Klocation), K

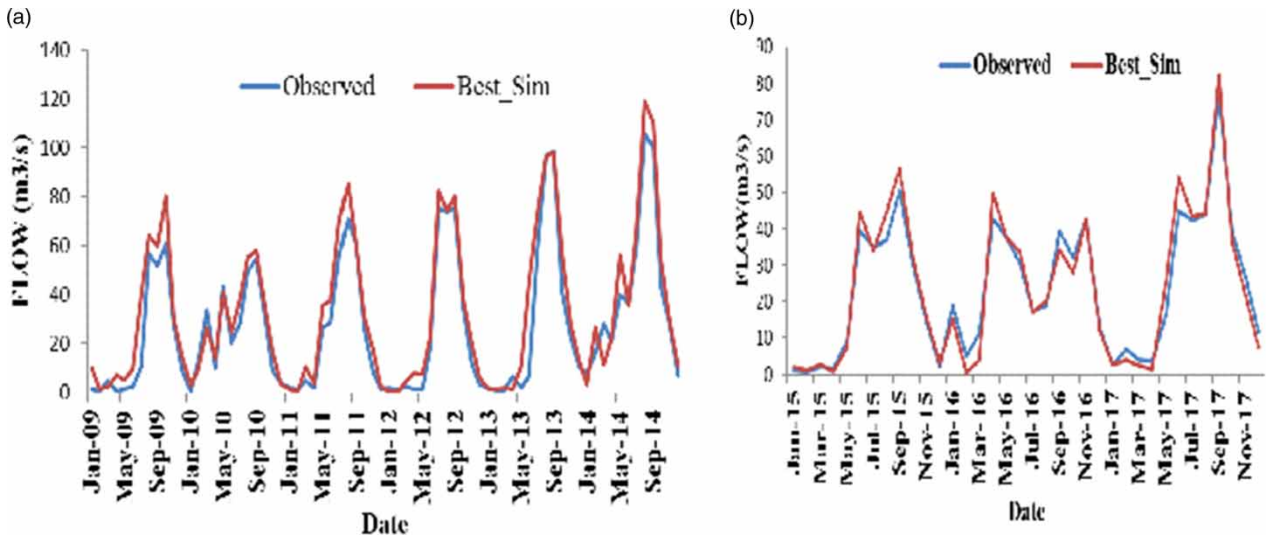

Figure 4 | Observed and simulated flow calibration (a) and validation (b) of 2018 LULC.

for standard (Kstandard) and K for stratum-level location (Klocationstrata) of 0.8510, 0.8613, 0.8712 and 0.8613, respectively. The K indexes were well above or near 85%. This result has a close agreement with the CA–Markov model validation comparison of the simulated and observed land use of 2015 which showed the K variation estimates of Kno (0.82), Kloc (0.82) and Kstandard (0.76) (Matlhodi *et al.* 2021). The K indexes indicated a high level of agreement between the reference and simulated map 2018, showing that the CA–Markov model is effective for predicting the future land uses in Bilate catchment.

LULC projection

The LULC is likely to change in the 2038 and 2058 periods compared to 2018 (Table 2; Figure 5). Compared with the LULC of 2018, water bodies, built-up areas and forest land are continuously increasing by 0.22–0.45%, 1.30–2.17% and 5.34–5.94%, respectively, while cultivation land is decreasing by 8.60–9.84%. Grazing and barren lands will increase from 2018 to 2038 by 0.12 and 1.53%, while the decrease from 2038 to 2058 is by 0.08 and 0.24%, respectively. The highest increment of forest/woodland is mainly related to Eucalyptus plantation at the expense of cultivation and grazing lands, and the practice of homestead agroforestry in the study catchment. This result was consistent with a recent study in Majang Forest Biosphere Reserves of Gambella, Southwestern Ethiopia, in which the CA–Markov model was employed (Tadese *et al.* 2021).

Climate change projections

Climate change projection was performed by using the ensemble mean of the models for the present (2021–2050) and mid (2051–2080) centuries under two emission scenarios relative to the baseline (1981–2010) over Bilate catchment. The projected changes in monthly rainfall and temperatures were put in the present (2021–2050) and mid (2051–2080) centuries under RCP4.5 and RCP8.5 emission scenarios relative to the base period (1981–2010).

Temperature projection

The mean monthly temperatures are expected to increase in the current (2021–2050) and mid (2051–2080) centuries compared to the baseline (1981–2010) (Figure 6). The maximum temperature in the present century (2021–2050) increased in the ranges of 0.3–1.2 and 0.8–1.5 °C under RCP4.5 and RCP8.5, respectively. The distribution of maximum temperature during the mid-century (2051–2080) increased in the ranges of 0.9–2.1 and 1.8–2.6 °C under RCP4.5 and RCP8.5, respectively. Similarly, the mean monthly minimum temperature was projected under RCP4.5 and RCP8.5 scenarios. The minimum temperature under RCP4.5 in the present (2021–2050) and mid (2051–2080) centuries increased in the ranges of 0.3–2.0 and 1.0–2.1 °C, respectively. Besides, RCP8.5 in the present (2021–2050) and mid (2051–2080) centuries increased in the ranges of 0.6–1.0 and 1.3–1.7 °C, respectively. It can be seen that the maximum and minimum temperatures of Bilate catchment in the mid-century are likely to become warmer than those in the present century under RCP4.5 and RCP8.5.

The projected change in temperature further upheld by McSweeney *et al.* (2012), Ministry of Foreign Affairs (2018) and Kebede *et al.* (2013) on climate change country profiles shows that the mean annual temperature is projected to increase by 1.1–3.1 °C by the 2060s and 1.5–5.1 °C by the 2090s. Similarly, the study by Kassie *et al.* (2013) showed that the annual mean temperature is expected to increase in the range of 1.4–4.1 °C by the 2080s in the Central Rift Valley of Ethiopia.

Table 2 | Projected LULC changes

LULC class (SWAT code)	Baseline LULC (%)	Predicted LULC (%)	
	2018	2038	2058
Water bodies (WATR)	0.34	0.45	0.47
Forest land (FRST)	22.02	27.55	28.50
Cultivation land (AGRC)	72.15	65.15	64.47
Built-up areas (URBN)	0.35	0.42	0.43
Grazing land (PAST)	0.49	0.63	0.57
Barren land (BARR)	4.65	5.80	5.56

The total area of the catchment is 562,560.39 ha.

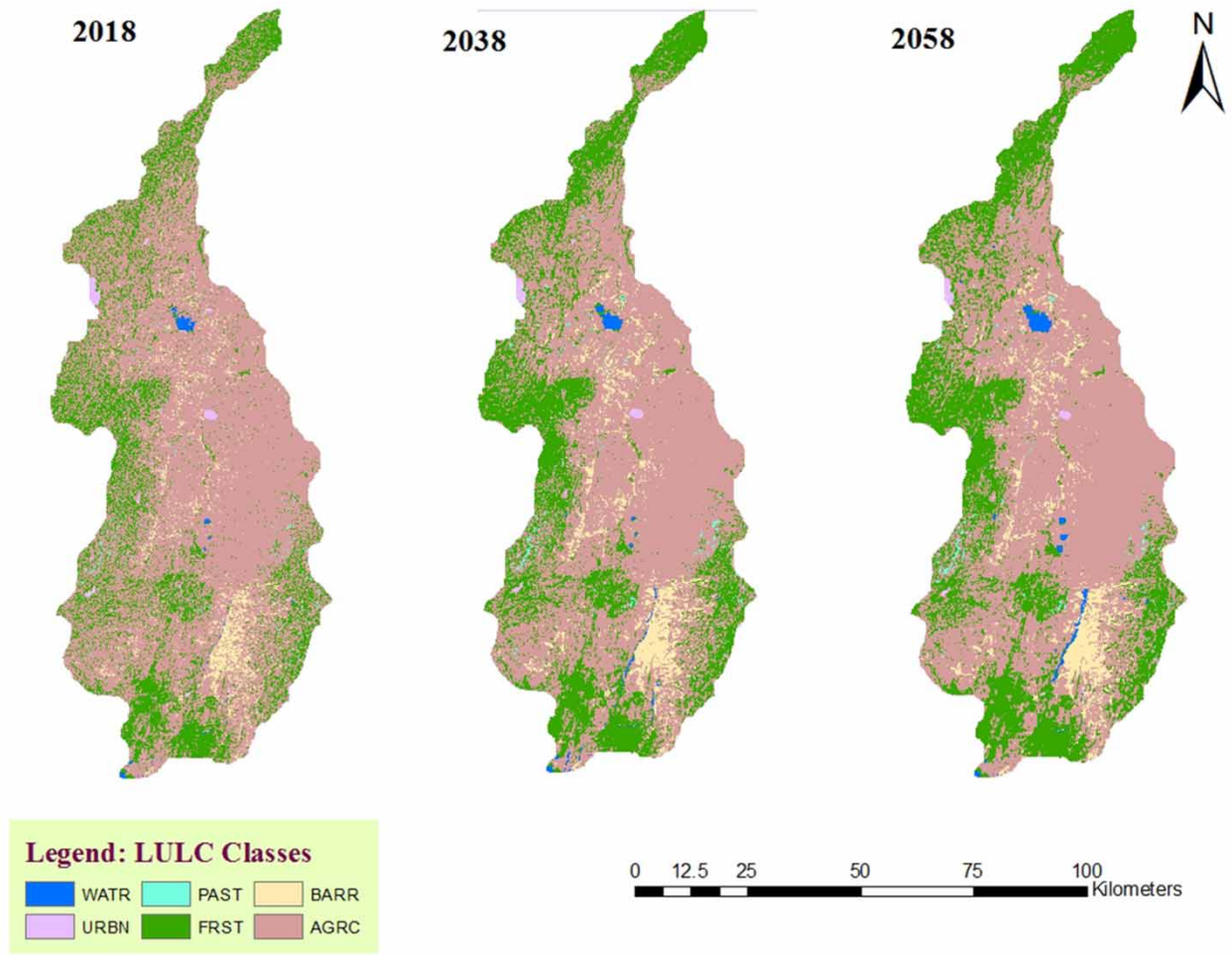

Figure 5 | LULC maps of 2018, 2038 and 2058.

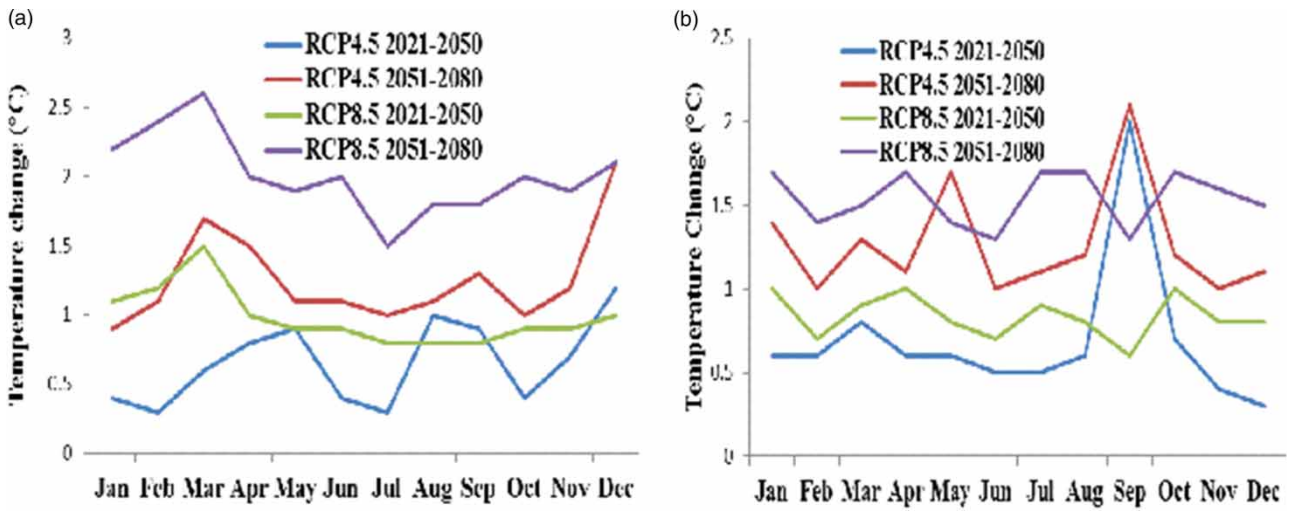

Figure 6 | Change in mean monthly maximum (a) and minimum (b) temperatures in 2021–2050 and 2051–2080 under RCP4.5 and RCP8.5 scenarios.

Rainfall projection

The projected change in rainfall during the present (2021–2050) and mid (2051–2080) centuries relative to baseline (1981–2010) under RCP4.5 and RCP8.5 scenarios of Bilate catchment was performed by using a multi-model ensemble of regional climate models. It seems that in the catchment, the rainfall is likely to feature increased and decreased under RCP4.5 and RCP8.5 scenarios (Figure 7). This is true especially over the catchment where rainfall is expected to decrease in the ranges of 134.4–659.4 and 38.7–822.5 mm under the RCP4.5 scenario, respectively, in the current (2021–2050) and mid (2051–2080) centuries. Similarly, rainfall is expected to decrease in the ranges of 74.9–624.2 and 52.0–436.3 mm under the RCP8.5 scenario, respectively, in the current (2021–2050) and mid (2051–2080) centuries. Rainfall is expected to decrease in January, March, May, June, July and August under RCP4.5 in two centuries. Besides, decreasing rainfall is projected in November under RCP4.5. Rainfall is expected to decrease in February, March, July, August and November under RCP8.5 in two centuries. In the mid-century, rainfall is projected to decrease in January, May and September under RCP8.5. Projected decreases in rainfall are more pronounced in the two centuries. For example, under RCP4.5 projected increase in rainfall is featured in September, October and December. Similarly, under RCP8.5 increased rainfall is featured in April, June and October.

The projected decrease in rainfall during the short rainy season (February–May) and the long rainy season (June–September) affects the catchment, because of subsistence rain-fed agriculture. Ethiopia's heavy dependence on rain-fed and subsistence agriculture increases its vulnerability to the adverse effects of climate changes (Kassa 2015; Zerga & Gebeyehu 2018). Water shortage is more pronounced in the forthcoming together with increasing temperature in the catchment. Studies in Ethiopia, climate trend analysis from 2010 to 2039 revealed rainfall decline ranges from 50 to 150 mm and is related to lower harvest and poor pastoral rangelands across the southern and eastern parts (Funk *et al.* 2012). Similarly, Kassie *et al.* (2013) reported that annual rainfall will change in the range of +10 to −40% by 2080, in which it will increase outside the growing season and decline during the growing seasons. Studies in Ethiopia reported unstable rainfall patterns and magnitudes in the future. For example, the future rainfall (2040–2059) of the long rainy season (June–September) tends to decrease over the southern part of the country (Li *et al.* 2015).

Hydrologic responses of the catchment

Hydrologic responses to 2018 LULC

The hydrologic components were simulated by the SWAT using climatic data from 2006 to 2017 and the 2018 LULC map. The SWAT model performed well in both the calibration and validation periods, accurately simulating the outlet flows at

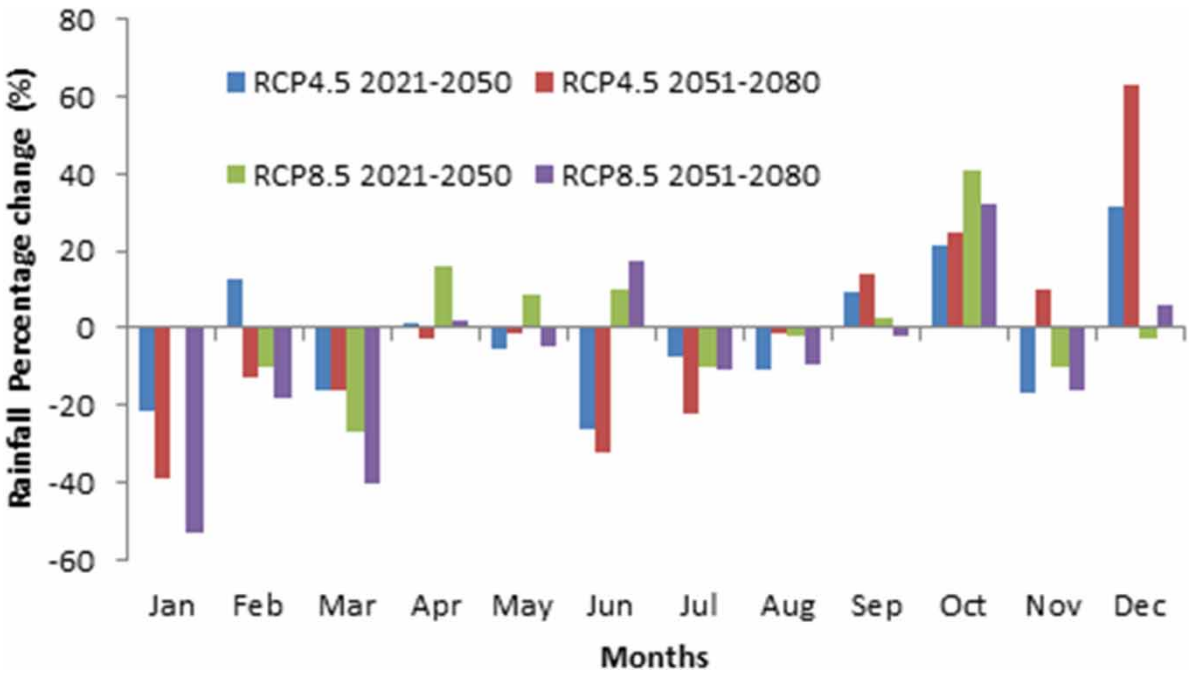

Figure 7 | Percentage change of rainfall in the Bilate catchment for 2021–2050 and 2051–2080 under RCP4.5 and RCP8.5 scenarios.

Halaba gauge station agreeing with model performance criteria (R^2 and NSE) after 12 parameters were optimized. During the calibration (2009–2014) and validation (2015–2017) periods, the time series plots of observed and simulated were matched in the periods (Figure 4). The model has been calibrated by river discharge; the hydrologic components such as potential evapotranspiration (PET), actual evapotranspiration (ET), surface runoff (SUR_Q), groundwater (GW_Q) and water yield (WYLD) were quantified. Notably, the simulated PET, ET, surface runoff, groundwater and water yield were 3,751.9, 1,537.98, 671.95, 637.16 and 1,401.34 mm/year, respectively, in 2018. The R^2 and NSE values in this study were generally good in calibration and validation. The result suggested that the SWAT model performed well and can replicate the catchment.

Future hydrologic responses to land-use change

To assess the impacts of LULC alteration on water balance, the calibrated model was used to simulate two LULC scenarios in 2038 and 3058 keeping the weather did not change. The water balance comparison was made between the 2018 and simulations under the future LULC scenarios (Table 3). The increase in surface runoff is 3.06, 3.78% for land use of 2038 and 2058, respectively. This increase in runoff can be attributed to a trend in cultivation land transformation to built-up areas and barren land increment. Groundwater and water yield are decreased by 1.85, 2.84%, and 1.83, 2.83%, respectively. The increase in PET is 6.34, 7.49% for land use in 2038 and 2058, respectively.

Many studies from different parts of the world confirmed that LULC changes significantly impact hydrologic processes. For example, Lu *et al.* (2015) found that in the land-use transformation, increased forest land area contributed more than any other land-use class to water yield, but built-up areas had the most impact due to small initial loss and infiltration. The finding agrees with Berihun *et al.* (2019) who reported that in Kecha and Kasiry, Upper Blue Nile Basin, the influence of land use has increased runoff by 4 and 28.7%, respectively.

Future hydrologic responses to climate changes

Changes in rainfall and temperature in the current (2021–2050) and mid (2051–2080) centuries were used to forecast the effects of climate change on hydrologic components of Bilate catchment. The calibrated and validated SWAT model was used to simulate future hydrologic components under RCP4.5 and RCP8.5 scenarios. The simulated hydrologic responses of the future periods and 2018 were compared to show their variations. SWAT simulations in two future periods showed a decrease in surface runoff, groundwater and water yield, while there was an increase in PET and ET (Table 4). The projected change in climate indicated a decline of rainfall and an increase of temperature in the catchment. Variations in the rainfall and temperature were associated to the variations in hydrologic response in Bilate catchment. Water yield, groundwater and surface runoff are likely to decrease under RCP4.5 and RCP8.5 in two future periods. These variations follow the path of rainfall changes (Table 4). An alteration in rainfall could result in variations in hydrologic responses. This is associated to the decrease in rainfall. For example, a 15.39% reduction in the annual rainfall caused about 9.22, 11.11 and 10.25% reductions in water yield, groundwater and surface runoff, respectively, under RCP4.5 in the mid (2051–2080) century. This result was similar to a recent study in Lake Tana Basin (Tigabu *et al.* 2020). PET and ET are expected to increase under RCP4.5 and RCP8.5 scenarios in two future periods. These changes follow the direction of temperature changes (Table 4). A 2.0 °C increase in the mean annual temperature resulted in about 19 and 13.9% increase in PET and ET, respectively, under RCP8.5 in the mid (2051–2080) century. This result agrees with a research report in Fincha watershed, Western Ethiopia (Dibaba *et al.* 2020).

The sensitivity of hydrologic components to climate change is different in future periods, and the impacts can be explained in the combination of the components. For example, the decline in rainfall reduced surface runoff, groundwater and water yield, while increasing temperature augmented an increase in PET and ET. The relationship between climate change and hydrologic components, ascertained by rainfall and temperature changes, varies with future periods under RCP4.5 and

Table 3 | Changes of the annual water balance under land-use changes

Land use	PET (%)	SUR_Q (%)	GW_Q (%)	WYLD (%)
2038	6.34	3.06	−1.85	−1.83
2058	7.49	3.78	−2.84	−2.83

Table 4 | Changes of the annual water balance under climate change

Scenario	Period	PET (%)	ET (%)	SUR_Q (%)	GW_Q (%)	WYLD (%)	Rainfall (%)	Mean temp. (°C)
RCP4.5	2021–2050	12	13.6	−7.15	8.22	−7.96	−27.11	0.7
	2051–2080	15	14	−10.25	−11.11	−9.22	−15.39	1.3
RCP8.5	2021–2050	14	14.7	−9.07	−10.46	−8.52	16.79	1.0
	2051–2080	19	13.9	−11.24	−12.54	−11.53	−46.26	2.0

RCP8.5 scenarios. For example, Mengistu *et al.* (2021) found that climate change in the Upper Blue Nile Basin in the 21st century showed an increase in PET by up to 27% under RCP8.5 and a decrease in water yield of 1.7 to 6.5% and 10.7 to 22.7% under RCP4.5 and RCP8.5, respectively. Berihun *et al.* (2019), in Kecha and Kasiry, Upper Blue Nile Basin, Ethiopia reported that the effect of climate change has increased evapotranspiration by 33.6 and 42.1%, respectively. Besides, a finding by Gebremeskel & Kebede (2018) in Tekeze River Basin reported that the effects of climate change will decrease surface runoff by 13 and 14%.

Climate change had a higher influence on water balance relative to that resulting from LULC change. Compared to LULC change, climate change leads to an increase in the average annual PET by 5.85 mm. However, the average annual SUR_Q, GW_Q and WYLD declined by 3.37, 3.33 and 2.57 mm, respectively. This result agrees with Kahsay *et al.* (2018) which reported a decline in groundwater followed by decreasing annual rainfall in Tekeze Basin, Ethiopia. Therefore, the hydrological processes are impacted more by climate change than the LULC change in Bilate catchment.

Future hydrologic responses to land-use and climate changes

The changes in LULC, temperature and rainfall were used to forecast the effects on water balance components in Bilate catchment. The hydrologic responses of the catchment to LULC and climate variations were investigated with two LULC scenarios. The first LULC scenario is from 2018–2038 and the second from 2018–2058 with the LULC of 2018. Two climate change periods are from 2021–2050 and 2051–2080 proposed under the RCP4.5 and RCP8.5 scenarios. The hydrologic responses of the Bilate catchment as considered to the annual PET, ET, SUR_Q, GW_Q and WYLD (Table 5).

The increasing temperature and decreasing rainfall under changing LULC in Bilate catchment resulted in a decline of runoff, groundwater and water yield, while there was an increase in PET and ET except under RCP4.5 of 2058 LULC. When LULC and climate variation scenarios are combined, the effects of water balance components are more noticeable. The highest annual surface runoff decline of 14.4% is projected under RCP4.5 in the mid-century, the highest groundwater decline of 16.8% is projected under RCP8.5 in the current century and the highest water yield decline of 14.1% is projected under RCP8.5 in the current century.

Studies conducted at different catchments agree with these results. The study by Yan *et al.* (2019) reported that the combined effect of LULC and climate has increased surface runoff, water yield and evapotranspiration. Similarly, Berihun *et al.* (2019) reported that the effect of climate and land-use variation had significantly increased surface runoff and evapotranspiration. Gebresilassie *et al.* (2020) found that the impact of land-use and climate variation has increased surface runoff and evapotranspiration under RCP8.5 from 2045 to 2055. In this study, the hydrologic components caused by combined effects of climate and land-use variations were higher than individual variation. This was further supported by Marhaento *et al.*

Table 5 | Change of the annual water balance under land-use and climate changes

Land use	RCPs	Period	PET (%)	ET (%)	SUR_Q (%)	GW_Q (%)	WYLD (%)
2038	RCP4.5	2021–2050	13.5	12.3	−11.6	−14.5	−13.7
2058	RCP4.5	2051–2080	−8.6	−7.2	−14.4	−15.2	8.5
2038	RCP8.5	2021–2050	15.5	13.9	−11.1	−16.8	−14.1
2058	RCP8.5	2051–2080	21.7	18.5	−12.4	−15.7	−13.5

(2018) that climate and land-use variations individually will cause water balance, but that more marked changes are likely if the factors are joined.

The spatial distribution of the hydrologic processes under projected climate and LULC changes of Bilate catchment is presented in Figures 8 and 9. The SWAT model showed that surface runoff, groundwater and water yields are high, while PET declined in the upstream areas in Bilate catchment. On the downstream areas, a significant amount of surface runoff, groundwater and water yield reduction was observed due to climate and land-use changes, although PET is significantly increasing. Moving downstream the water potential is reduced due to high temperature increase coupled with decreasing rainfall that could lead to reduced soil moisture, which is required for plant growth. Besides, semi-aridity is another problem for the downstream areas in Bilate catchment. This could imply the reduced availability of water for crop production, which will become a continuing problem for the farmers in the catchment whose livelihood is based on agriculture.

CONCLUSION

This study investigated the effects of climate and LULC variations on the hydrologic components in Bilate catchment, Rift Valley Basin of Ethiopia. Two climate and LULC alteration scenarios were established, and the hydrologic components were simulated using the SWAT model. LULC scenario prediction maps of 2038 and 2058 were generated using the CA–Markov model. Climate changes for the current (2021–2050) and mid (2051–2080) centuries were projected using the ensemble mean of regional climate models under RCP4.5 and RCP8.5 scenarios. The model was calibrated, validated for 2018 and used to simulate the forthcoming water balance under two scenarios. The agreement between the measured and replicated river flows indicated that the SWAT model could be used to simulate the hydrologic responses to climate and LULC variations in the catchment. Besides, the forthcoming water balances were associated with those of 2018.

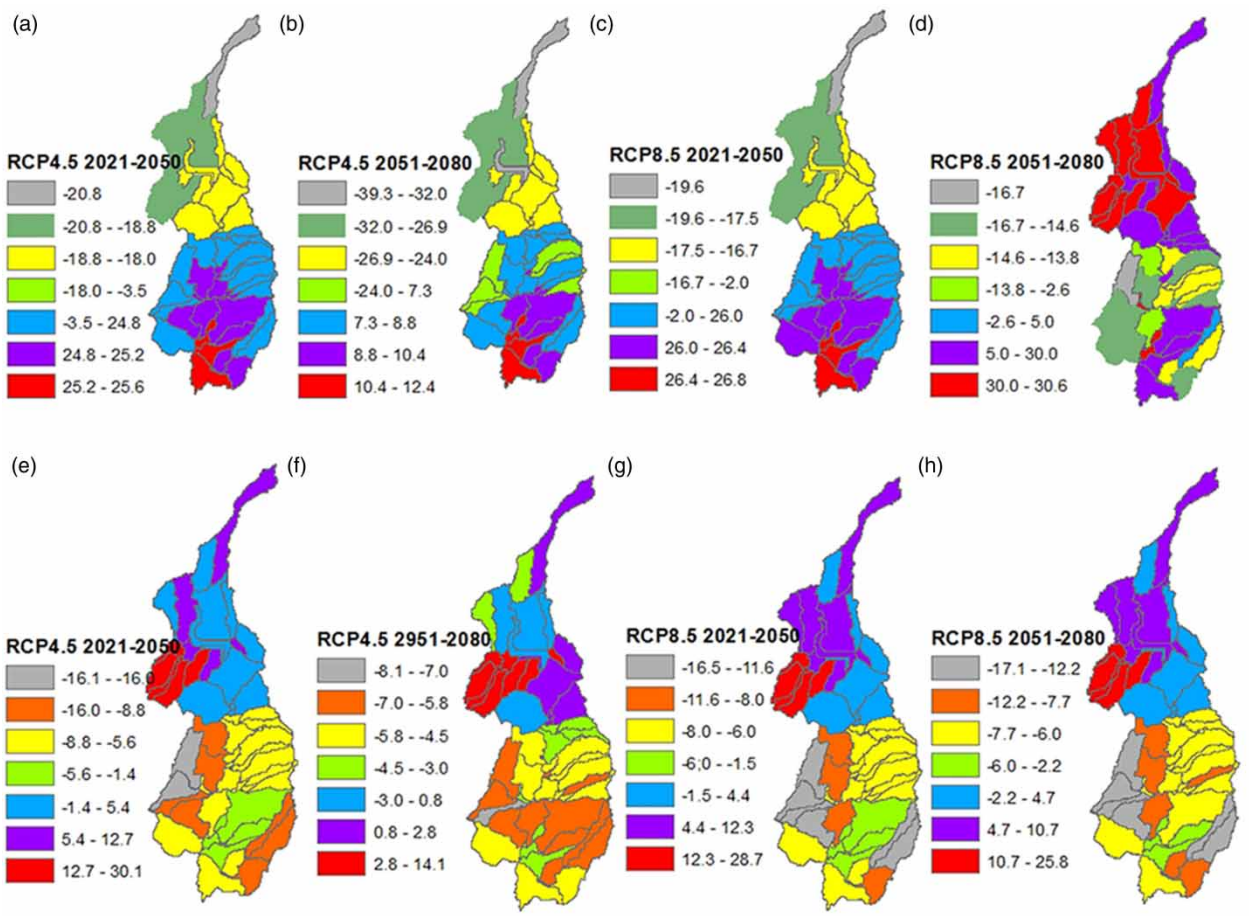

Figure 8 | Spatial distribution of water balance: PET (a–d) and SUR_Q (e–h) under combined land-use and climate changes.

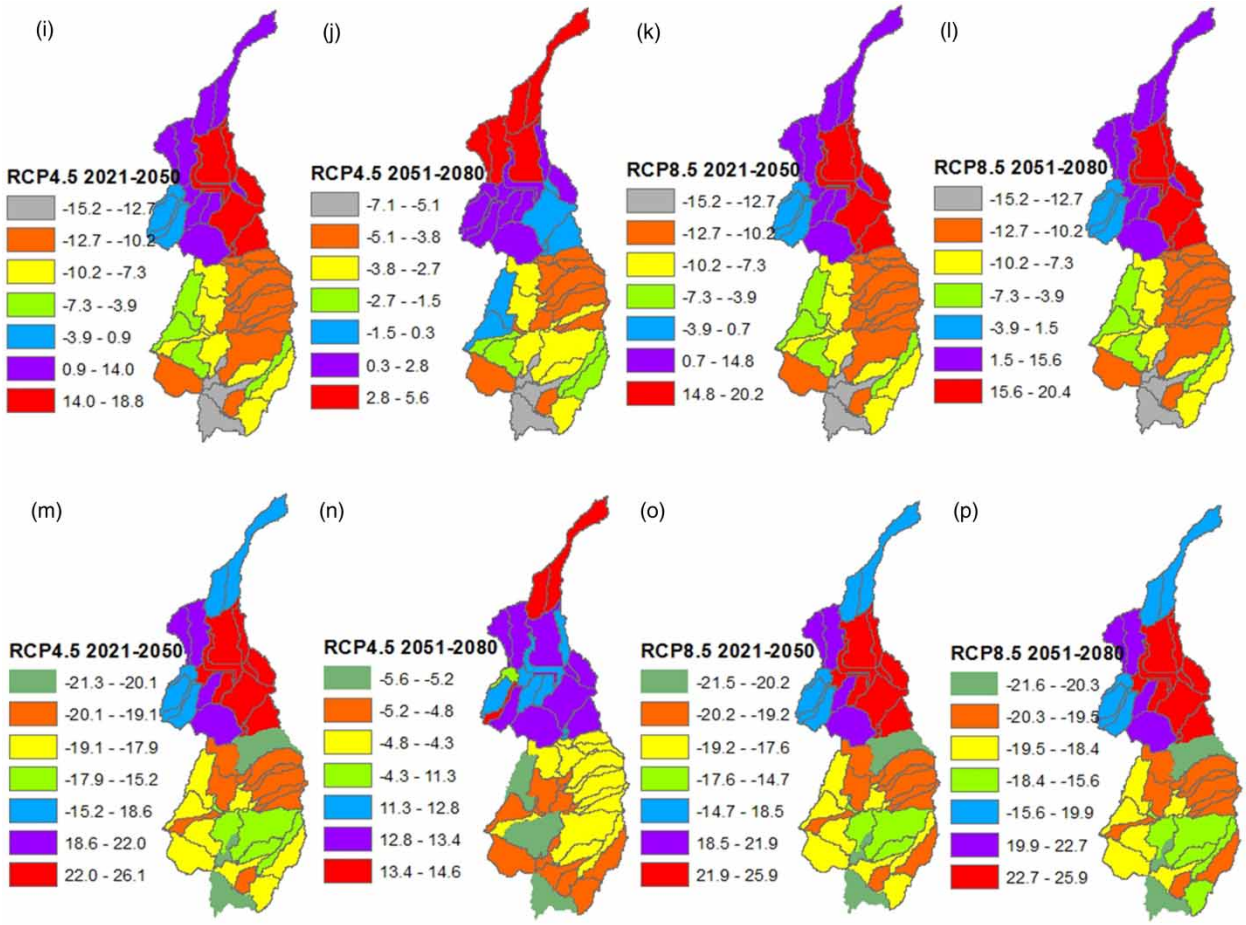

Figure 9 | Spatial distribution of water balance: GW_Q (i–l) and WYLD (m–p) under combined land-use and climate changes.

The historical and forthcoming hydrologic responses were simulated under the monthly scales. Runoff, water yield and groundwater decreased in the current (2021–2050) and mid (2051–2080) centuries under the RCP4.5 and RCP8.5, but water yield increased in the current century under the RCP4.5 scenario. PET and ET increased in two periods, but decreased in the mid-century under the RCP4.5 scenario. The hydrologic responses follow the path of rainfall. This is related to the decline in rainfall amount in Bilate catchment. The decline in the rainfall resulted in a significant decline in surface runoff, water yield and groundwater. Similarly, the hydrologic responses follow the path of temperature in the catchment. This is attributed to the increasing temperature in Bilate catchment. The likely increase in the mean temperature resulted in a substantial increase in ET and PET. The combined impacts of climate and LULC variations on hydrologic responses in the forthcoming are greater than the variation trends of climate or LULC change alone. Besides, the effect of climate change on water balance is higher than that of LULC change.

Furthermore, the decreasing rainfall and increasing temperature in the catchment may cause hot and dry years. Accordingly, the catchment is highly vulnerable to climate change and its impacts could range from warming to crop failures. The change in water balance in Bilate catchment is likely to be more challenging in the future.

The study suggests that the assessment of the combined impact of climate and LULC changes on hydrologic responses in Bilate catchment is well represented by the SWAT simulations. However, the feature of hydro-climatic data and the lack of local LULC evidence in the region need urgent attention to improve our understanding of the variations in the future.

The results provided evidence on how the hydrological processes in Bilate catchment respond to the changes in climate and LULC. This could help to plan water resources and land management interventions. If the degraded sloppy lands are rehabilitated, tree plantations are based on decisions as to how soil and water conservation works properly implemented the groundwater recharge increase. Accordingly, the surface runoff which washes the topsoil and nutrients into the water bodies is reduced. Furthermore, Lake Abaya in the catchment should be buffered with proper management strategies.

Overall, the result highlights the need for concerned bodies to urge strong climate-resilient management strategies and counteract the climate changes in Bilate catchment.

ACKNOWLEDGEMENTS

We would like to thank Jimma and Wolaita Soddo Universities for providing materials and resource supports for the study. The authors are pleased to thank the USGS for the provision of Landsat data. It is our pleasure to thank Desalegn Borsamo, who helped us with English language editing.

DATA AVAILABILITY STATEMENT

All relevant data are included in the paper or its Supplementary Information.

REFERENCES

Abbaspour, K. C., Yang, J., Maximov, I., Siber, R., Bogner, K., Mieleitner, J., Zobrist, J. & Srinivasan, R. 2007 Spatially distributed modelling of hydrology and water quality in the pre-alpine/alpine Thur watershed using SWAT. *Journal of Hydrology* **333**, 413–430. https://doi.org/10.1016/j.jhydrol.2006.09.014.

Adugna, A. 2014 *Demography and Health: Livelihood Profiles Regional Overview*. SNNPR. Available from: https://www.ethdemographyandhealth.org.

Al-sharif, A. A. A. & Pradhan, B. 2014 Monitoring and predicting land use change in Tripoli Metropolitan City using an integrated Markov chain and cellular automata models in GIS. *Arabian Journal of Geosciences* **7**, 4291–4301. https://doi.org/10.1007/s12517-013-1119-7.

Arnold, J. G., Srinivasan, R., Muttiah, R. S. & Williams, J. R. 1998 Large area hydrologic modeling and assessment part I: model development. *Journal of the American Water Resources Association* **34** (1), 73–89. https://doi.org/10.1111/j.1752-1688.1998.tb05961.x.

Berihun, M. L., Tsunekawa, A., Haregeweyn, N., Meshesha, D. T., Adgo, E., Tsubo, M., Masunaga, T., Fenta, A. A., Sultan, D., Yibeltal, M. & Ebabu, K. 2019 Hydrological responses to land use/land cover change and climate variability in contrasting agro-ecological environments of the Upper Blue Nile Basin, Ethiopia. *Science of the Total Environment* **689**, 347–365. https://doi.10.1016/j.scitotenv.2019.06.338.

Bessah, E., Raji, A. O., Taiwo, O. J., Agodzo, S. K., Ololade, O. O. & Strapasso, A. 2020 Hydrological responses to climate change and land use changes: the paradox of regional and local climate effect on Para River Basin of Ghana. *Journal of Hydrology: Regional Studies* **27** (100654), 1–12. http://doi.org/1-.1016/j.ejrh.2019.100654.

Biniyam, Y. & Kemal, A. 2017 The impacts of climate change on rainfall and flood frequency: the case of Hare watershed, Southern Rift Valley of Ethiopia. *Journal of Earth Science & Climatic Change* **8** (383), 1–5. doi:10.4172/2157-7617.1000383.

Boru, G. F., Gonfa, Z. B. & Diga, G. M. 2019 Impacts of climate change on stream flow and water availability in anger sub-basin, Nile Basin of Ethiopia. *Sustainability of Water Resources Management* **5**, 1755–1764. https://doi.org/10.1007/s40899-019-00327-0.

Castro, C. L., PielkeSr, R. A. & Leoncini, G. 2005 Dynamical downscaling: assessment of value retained and added using the Regional Atmospheric Modeling System (RAMS). *Journal of Geophysical Research* **110**, 1–21. https://doi.10.1029/2004JD004721.

Chai, T. & Draxler, R. R. 2014 Root mean square error (RMSE) or mean absolute error (MAE)? – Arguments against avoiding RMSE in the literature. *Geoscientific Model Development* **7**, 1247–1250. https://doi.org/10.5194/gmd-7-1247-2014.

Conway, D. & Schipper, E. L. F. 2010 Adaptation to climate change in Africa: challenges and opportunities identified from Ethiopia. *Global Environmental Change* **21**, 227–237.

CSA 2013 *Central Statistical Agency: Population Projection of Ethiopia for All Regions at Wereda Level from 2014–2017*. Federal Democratic Republic of Ethiopia Central Statistical Agency, Addis Ababa, Ethiopia. https://www.academia.edu/30252151/Federal_Democratic_Republic_of_Ethiopia_Central_Statistical_Agency_Population_Projection_of_Ethiopia_for_All_Regions_At_Wereda_Level_from_2014_2017

Dibaba, W. T., Demissie, T. A. & Miegel, K. 2020 Watershed hydrological response to combined land use/land cover and climate change in highland Ethiopia: Finchaa catchment. *Water* **12** (1801), 1–25. https://doi.org/10.3390/w12061801.

Eastman, J. R. 2016 *IDRISI Terrset Manual*. IDRISI Production, Worcester, MA, USA.

FAO 2002 *Major Soils of the World Land and Water Digital Media Series; CD-ROM*. Food and Agricultural Organization of the United Nations, Rome, Italy.

Feyereisen, G. W., Strickland, T. C., Bosch, D. D. & Sullivan, D. G. 2007 Evaluation of SWAT manual calibration and input parameter sensitivity in Little River Watershed. *American Society of Agricultural and Biological Engineers* **50** (3), 843–855.

Flato, G., Marotzke, J., Abiodun, B., Braconnot, P., Chou, S. C., Collins, W., Cox, P., Driouech, F., Emori, S., Eyring, V., Forest, C., Gleckler, P., Guilyardi, E., Jakob, C., Kattsov, V., Reason, C. & Rummukainen, M. 2013 Evaluation of climate models. In: *Climate Change 2013: The Physical Science Basis. Contribution of Working Group I to the Fifth Assessment Report of the Intergovernmental Panel on Climate Change* (Stocker, T. F., Qin, D., Plattner, G.-K., Tignor, M., Allen, S. K., Doschung, J., Nauels, A., Xia, Y., Bex, V. & Midgley, P. M., eds). Cambridge University Press, pp. 741–882. doi:10.1017/CBO9781107415324.020.

Funk, C., Rowland, J., Kebede, E. & Biru, N. A. 2012 Climate trend analysis of Ethiopia. FEWNET (Famine Early Warning System Network), 1–6.

Gebremeskel, G. & Kebede, A. 2018 Estimating the effect of climate change on water resources: integrated use of climate and hydrological models in the Werti watershed of the Tekeze River Basin, Northen Ethiopia. *Agriculture and Natural Resources* **52**, 195–207. https://doi.org/10.1016/j.anres.2018.06.010.

Gebresilassie, A., Taddele, Y. D., Hailu, D., Bayabil, H. & Sisay, K. 2020 Impacts of climate and land use change on hydrological responses in Gumara watershed, Ethiopia. pp. 1–24. Available from: https://www.authorea.com/doi/pdf/10.22541/au.159863388.81259725/v1 (accessed 29 May 2021).

Germer, S., Neill, C., Vetter, T., Chaves, J., Krusche, A. V. & Elsenbeer, H. 2009 Implications of long-term land use change for the hydrology and solute budgets of small catchment in Amazonia. *Journal of Hydrology* **364** (3/4), 349–363.

Getachew, B., Manjunatha, B. R. & Bhat, H. G. 2021 Modeling projected impacts of climate and land use/land cover changes on hydrological responses in the Lake Tana Basin, upper Blue Nile River Basin, Ethiopia. *Journal of Hydrology* **595**, 125974. https://doi.org/10.1016/j.jhydrol.2021.125974.

Gidey, E., Dikinya, O., Sebego, R., Segosebe, E. & Zenebe, A. 2017 Cellular automata and Markov chain (CA_Markov) model-based predictions of future land use and land cover scenarios (2015-2033) in Raya, northern Ethiopia. *Modeling Earth Systems and Environment* **3** (10), 1245–1262. https://doi.org/10.1007/s40808-017-0397-6.

Giorgi, F., Jones, C. & Asrar, G. 2009 Addressing climate information needs at the regional level: the CORDEX framework. *WMO Bulletin* **58** (3), 175–183.

Kahsay, K. D., Pingalea, S. M. & Hatiyea, S. D. 2018 Impact of climate change on groundwater recharge and base flow in the subcatchment of Tekeze basin, Ethiopia. *Groundwater for Sustainable Development* **6**, 121–133. https://doi.org/10.1016/j.gsd.2017.12.002.

Kassa, F. 2015 Ethiopian seasonal rainfall variability and prediction using canonical correlation analysis (CCA). *Earth Science* **4** (3), 112–119. https://doi.org/10.11648/j.earth.20150403.14.

Kassie, B. T., Rotter, R. P., Hengsduk, H., Asseng, S., Vanittersum, M. K., Kahiluoto, H. & Van Keulen, H. 2013 Climate variability and change in the Central Rift Valley of Ethiopia: challenges for rainfed crop production. *Journal of Agricultural Science*, 1–17. https://doi.org/10.1017/S0021859612000986.

Kebede, A., Diekkruger, B. & Moges, S. A. 2013 An assessment of temperature and precipitation change projections using a regional and a global climate model for the Baro-Akobo Basin, Nile Basin, Ethiopia. *Journal of Earth Science & Climatic Change* **4** (133), 1–12. doi:10.4172/2157-7617.1000133.

Kim, I., Jeong, G., Park, S. & Tenhunen, J. 2011 Predicted land use change in the Soyang River Basin, South Korea. In: *Proceedings of the TERRECO Science Conference*, Garmisch-Partenkirchen, Germany, pp. 17–24.

Lamparter, G., Nobrega, R., Kovacs, K., Amorim, R. S. & Gerold, G. 2019 Modeling hydrological impacts of agricultural expansion in two macro catchments in Southern Amazonia, Brazil. *Regional Environmental Change* **18** (1), 91–103. http://dx.doi.org/10.1007/s10113-016-1015-2.

Leander, R. & Buishan, T. A. 2007 Resampling of regional climate model output for the simulation of extreme river flows. *Journal of Hydrology* **332**, 487–496. doi:10.1016/j.jhydrol.2006.08.006.

Leander, R., Adri Buishand, T., van den Hurk, B. J. J. M. & de Wit, M. J. M. 2008 Estimated changes in flood quantiles of therivermeuse from resampling of regional climate model output. *Journal of Hydrology* **351**, 331–343. doi:10.1016/j.jhydrol.2007.12.020.

Legesse, D., Abiye, T. A. & Vallet-Coulomb, C. 2010 Modeling impacts of climate and land use changes on catchment hydrology: Meki River, Ethiopia. *Hydrology and Earth System Sciences Discussions* **7**, 4535–4565.

Li, Z., Liu, W., Zhang, X. & Zheng, F. 2009 Impacts of land use change and climate variability in an agricultural catchment on the Loess Plateau of China. *Journal of Hydrology* **377**, 35–42. https://doi.org/10.1016/j.jhydrol.2009.08.007.

Li, L., Li, W., Ballard, Y., Sun, G. & Jeuland, M. 2015 CMIP5 model simulations of Ethiopian Kiremt-season precipitation: current climate and future changes. *Climate Dynamics* **46**, 2883–2895. https://doi.org/10.1007/s00382-015-2737-4 (accessed 21 July 2021).

Liu, J., Xue, B. & Yan, Y. 2020 The assessment of climate change and land-use influence on the runoff of a tropical coastal basin in Northern China. *Sustainability* **12** (10050), 1–13. https://doi.org/10.3390/su122310050.

Lu, Z., Zou, S., Qin, Z., Yang, Y., Xiao, H., Wei, Y., Zhang, K. & Xie, J. 2015 Hydrologic responses to land use change in the loess plateau:case study in the Upper Fenhe River Watershed. *Advances in Meteorology* **676030**, 1–10. http://dx.doi.org/10.1155/2015/676030.

Lutz, A., Immerzed, W., Biemans, H., Maat, H., Veldore, V. & Shretha, A. 2016 *Selection of Climate Models for Developing Representative Climate Projections for the Hindu Kush Himalayan Region*. HI-AWARE Working Paper 1, p. 46, Kathmandu, Nepal.

Marhaento, H., Boodij, M. J. & Hoekstra, A. Y. 2018 Hydrological changes to future land use change and climate change in a tropical catchment. *Hydrological Sciences Journal* **63** (9), 1368–1385. https://doi.org/10.1080/02626667.2018.1511054.

Mascaro, G., White, D. D., Westerhof, P. & Bliss, N. 2015 Performance of the CORDEX-Africa regional climate simulations in representing the hydrological cycle of the Niger River basin. *Journal of Geophysical Research Atmospheres* **12**, 425–444. https://doi.org/10.1002/2015JD023905.

Matlhodi, B., Kenabatho, P. K., Parida, B. P. & Maphanyane, J. G. 2021 Analysis of the future land use land cover changes in the Gaborone dam catchment using CA-Markov model: implications on water resources. *Remote Sensing* **13**, 2427. https://doi.org/10.3390/rs13132427.

McSweeney, C., New, M. & Lizcano, G. 2012 *Climate Change Country Profile*. UNDP, Ethiopia. pp. 1–27. Available from: https://digital.library.unt.edu/ark:/67531/metadc226682/m1/ (accessed 21 July 2021).

Mengistu, D., Woldeamlak, B., Dosio, A. & Panitz, H. 2021 Climate change impacts on water resources in the Upper Blue Nile (Abay) River Basin, Ethiopia. *Journal of Hydrology* **592**, 125614. JRC117717. http://dx.doi.org/10.1016/j.jhydrol.2020.125614.

Ministry of Forien Affaisr 2018 *Climate Change Profile: Greater Horn of Africa*. Ministry of Foreign Affairs of the Neatherlands, Hague, The Neatherlands, pp. 1–20. Available from: http://country-profiles.geog.ox.ac.uk (accessed 21 July 2021).

Mohammed, A. K. 2013 *The Effect of Climate Change on Water Resources Potential of Omo Gibe Basin, Ethiopia*. PhD Thesis, Germany, Universitat der Bundeswehr München.

Moriasi, D. N., Arnold, J. G., Van Liew, M. W., Bingner, R. L., Harmel, R. D. & Veith, T. L. 2007 Mode evaluation guidelines for systematic quantification of accuracy in watershed simulation. *American Society of Agricultural and Biological Engineers* **50**, 885–900. doi:10.13031/2013.23153.

Mosammam, H. M., Nia, J. T., Khani, H., Teymouri, A. & Kazemi, M. 2016 Monitoring land use change and measuring urban sprawl based on its spatial forms: the case of Qom city. *The Egyptian Journal of Remote Sensing and Space Sciences* **20** (1), 103–116. https://doi.org/10.1016/j.ejrs.2016.08.002.

MoWIE 2019 *Bilate River Flow Data from 2006-2017*. Ministry of Water, Irrigation and Energy of Ethiopia.

Nash, J. E. & Sutcliffe, J. W. 1970 River flow forecasting though conceptual models: part I. A discussion of principles. *Journal of Hydrology* **10** (3), 282–290. http://dx.doi.org/10.1016/0022-1694 (70)90255-6.

Ndulue, E. L. & Mbajiorgu, C. C. 2018 Modeling climate and land use change impacts on streamflow and sediment yield of an agricultural watershed using SWAT. *AgricEngInt: CIGR Journal* **20** (4), 15–25.

Negesse, A. 2021 Impacts of land use and land cover change on soil erosion and hydrological responses in Ethiopia. *Applied and Environmental Soil Sciences* **2021**, 1–10. https://doi.org/10.1155/2021/6669438.

Neitsch, S. L., Arnold, J. R., Kiniry, J. R. & Williams, J. R. 2011 *Soil and Water Assessment Tool Theoretical Documentation Version 2009*. AgriLife Research and Extension. Technical Report 406, Texas Water Resources Institute, Texas. Available from: https://hdl.handle.net/1969.1/128050 (accessed 9 June 2021).

Nikulin, G., Jones, C., Giorgi, F., Asrar, G., Büchner, M., Cerezo-Mota, R., Christensen, O. B., Deque, M., Fernandez, J., Hänsler, A., Van Meijgaard, E., Samuelsson, P., Sylla, M. B. & Sushama, L. 2012 Precipitation climatology in an ensemble of CORDEX-Africa regional climate simulations. *Journal of Climate* **25**, 6057–6078. https://doi.10.1175/JCLI-D-11-00375.1.

NMSA 2019 *The National Meteorological Services Agency of Ethiopia*.

Nouri, J., Gharagozlou, A., Arjmandi, R., Faryadi, S. & Adl, M. 2014 Predicting urban land use changes using a CA-Markova model. *Arabian Journal of Scientific and Engineering Research* **39**, 5565–5573.

Pan, S., Liu, D., Wang, Z., Zhao, Q., Zou, H., Hou, Y., Liu, P. & Xiong, L. 2017 Runoff responses to climate and land use/cover changes under future scenarios. *Water* **9** (475), 1–23. https://doi.org/10.3390/w9070475.

Pontius, R. G. & Millones, M. 2011 Death to Kappa: birth of quantity disagreement and allocation disagreement for accuracy assessment. *International Journal of Remote Sensing* **32**, 4407–4429. http://dx.doi.org/10.1080/01431161.2011.552923.

Qiu, Y. & Lu, J. 2018 Dynamic simulation of Spartina alterniflora based on CA-Markov model – a case study of Xiangshan bay of Ningbo City, China. *Aquatic Invasions* **13** (2), 299–309. https://doi.org/10.3391/ai.2018.13.2.10.

Santhi, C., Arnold, J. G., Williams, J. R., Dugas, W. A., Srinivasan, R. & Hauck, L. M. 2001 Validation of the SWAT model on a large river basin with point and nonpoint sources. *Journal of the American Water Resources Association* **37**, 1169–1188. https://doi.org/10.1111/j.1752-1688.2001.tb03630.x.

Shooshtari, S. J., Shayesteh, K., Gholamalifard, M., Azari, M., Serrano-Notivoli, R. & Lopez-Moreno, J. I. 2017 Impacts of future land cover and climate change on water balance in Northern Iran. *Hydrological Sciences Journal* **62** (16), 2655–2673. https://doi.org/10.1080/02626667.2017.1403028.

Tadese, S., Soromessa, T. & Tesefaye Bekele, T. 2021 Analysis of the current and future prediction of land use/land cover change using remote sensing and the CA-Markov model in Majang Forest Biosphere Reserves of Gambella, Southwestern Ethiopia. *The Scientific World Journal* **2021**, 1–18. https://doi.org/10.1155/2021/6685045.

Talebizadeh, M., Morid, S., Ayyoubzadeh, S. A. & Ghasemzadeh, M. 2009 Uncertainty analysis in sediment load modeling using ANN and SWAT model. *Water Resources Management* **24**, 1747–1761. Available from: https://doi.org/10.1007/s11269-009-9522-2.

Teklay, A., Dile, Y. T., Asfaw, D. H., Bayabil, H. K. & Sisay, K. 2021 Impacts of climate and land use change on hydrological response in Gumara Watershed, Ethiopia. *Ecohydrology and Hydrobiology* **21** (2), 315–332. https://doi.org/10.1016/j.ecohyd.2020.12.001.

Terink, W., Hurkmans, R. T. W. L., Torfs, P. J. J. F. & Uijlenhoet, R. 2009 Bias correction of temperature and precipitation data for regional climate model application to the Rhine basin. *Hydrology and Earth System Sciences Discussions* **6**, 5377–5413.

Tigabu, T. B., Wagner, P. D., Hormann, G., Kiesel, J. & Fohrer, N. 2020 Climate change impacts on the water and groundwater resources of the Lake Tana Basin, Ethiopia. *Journal of Water and Climate Change* **877599**, 1–20. https://doi.org/10.2166/wcc.2020.126.

Tinghai, O., Deliang, C., Hans, W. L. & Jee-Hoon, J. 2013 Evaluation of global climate models in simulating extreme precipitation in China. *Tellus A: Dynamic Meteorology and Oceanograph* **15** (19799), 1–16. http://dx.doi.org/10.3402/tellusa.v65i0.19799.

Viera, A. J. & Garret, J. M. 2005 Understanding interobserver agreement: the Kappa statistics. *Family Medicine* **37** (5), 360–363.

Woldesenbet, T. A., Elagib, N. A., Ribbe, L. & Heinrich, J. 2018 Catchment response to climate and land use changes in the Upper Blue Nile Sub-basin, Ethiopia. *Science of the Total Environment* **644**, 193–206. https://doi.org/10.1016/j.scitotenv.2018.06.198.

Worner, V., Kreye, P. & Meon, G. 2019 Effects of bias-correcting climate model data on the projection of future changes in high flows. *Hydrology* **6** (46), 1–17. doi:10.3390/hydrology6020046.

Yan, R., Cai, Y., Li, C., Wang, X. & Liu, Q. 2019 Hydrological responses to climate and land use changes in a watershed of the Loess Plateau, China. *Sustainability* **11** (5), 1–9. https://doi.org/10.3390/su11051443.

Yin, J., He, F., Xiong, Y. J. & Qiu, G. Y. 2017 Effects of land use/land cover and climate changes on surface runoffin a semi-humid and semi-arid transition zone in northwest China. *Hydrology of Earth System Sciences* **21**, 183–196. https://doi.org/10.5194/hess-21-183-2017.

Zerga, B. & Gebeyehu, G. 2018 Climate change in Ethiopia variability, impact, mitigation, and adaptation. *Journal of Social Science and Humanities Research* **2** (4), 1–20. doi:10.13140/RG.2.2.16782.46408.

Zhang, L., Wang, C., Liang, G., Cui, Y. & Zhang, Q. 2020 Influence of land use change on hydrological cycle: application of SWAT to Su-Mi-Huai area in Beijing, China. *Water* **12** (11), 1–17. https://doi.org/10.3390/w12113164.

Zuo, D., Xu, Z., Yao, W., Jin, S., Xiao, P. & Ran, D. 2016 Assessing the effect of changes in land use and climate on runoff and sediment yields from a watershed in the Loess Plateau of China. *Science of the Total Environment* **544**, 238–250. https://doi.org/10.1016/j.scitotenv.2015.11.060.

First received 21 July 2021; accepted in revised form 10 September 2021. Available online 28 September 2021